Chapter 2

Static Experimental Technique

Contact resistance measurements were made using a physically stationary, thermally transient technique. Time temperature responses were measured for a system with a metal – plastic interface. The measured response was then compared with a predicted response to obtain a total resistance value using statistical techniques. As the thickness and thermal conductivity of the plastic was known, the contact resistance could be determined.

2.1 Background and Derivation

The test procedure for the initial experimental phase is similar to the one outlined by Beckman and Mitchell (1969) for measuring the thermal conductivity of paint. In the present study, two blocks at different initial temperatures with a known weight on the top block were brought together with the plastic between them. The blocks were insulated on all remaining sides. From the resulting temperature time profile of the two block system, the total thermal resistance between the blocks was determined. The total resistance between the blocks consists of the conduction through the plastic sample and two contact resistances of the plastic – aluminum interface. The contact resistance was assumed to be the same at each interface. Relating the measured resistance to the contact resistance:

$$R''_{Total} = R''_{contact} + \frac{L_{sample}}{k_{sample}} + R''_{contact} \tag{2.1.1}$$

A lumped thermal capacitance model was used to derive an analytical expression for the temperature vs. time responses of the two blocks placed in contact during the experiment. The lumped mass approach assumed the blocks to be isothermal, but at different temperatures for each block. The plastic sample between the blocks was assumed to have negligible thermal capacitance, but its resistance to steady state heat flow is considered. All considered heat flows are shown in figure 2.1.1 below:

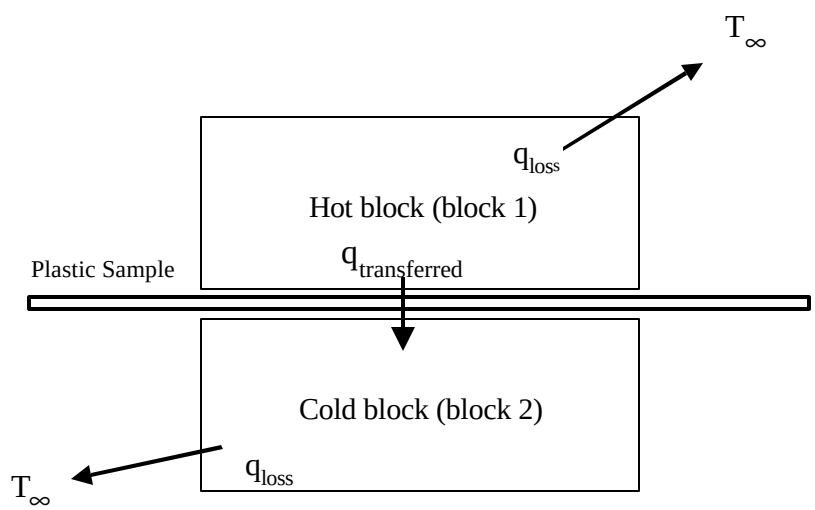

Figure 2.1.1: Heat Flows in Experimental Setup.

Over time the energy in the hot block is conducted through the plastic to the cold block and also conducted through the insulation to the surroundings. The cold block gained thermal energy from the hot block and lost energy by conduction through the insulation and to the surroundings. The heat flows of each block can be modeled with a first order differential equation. When the blocks are placed in contact, the differential equations of the two blocks are coupled, and must be solved simultaneously.

2.2 Lumped Capacitance Technique

The energy balance for a block can be represented by a model having the differential equation relating the energy increase (or decrease) of a block to the heat loss from the block to the surroundings and the energy transfer between the blocks. For each block the Energy balance related the energy inflows and outflows to the internal energy change of the blocks. For both blocks:

$$\dot{E}_{in} - \dot{E}_{out} = \frac{dE}{dt} \tag{2.2.1}$$

The energy out for both blocks was expressed as:

$$\dot{E}_{out} = h_{block} \cdot A_{surface} \cdot (T_{block} - T_{\infty}) \tag{2.2.2}$$

The hot block was considered block 1, and the cold block was block 2. For the hot block the energy transferred to the cold block was also a loss:

$$\dot{E}_{out} = \frac{A_{contact}}{R''_{total}} \cdot (T_1 - T_2) \tag{2.2.3}$$

The energy in for the cold block was:

$$\dot{E}_{in} = \frac{A_{contact}}{R''_{total}} \cdot (T_1 - T_2) \tag{2.2.4}$$

The mechanism equations were related to form the differential equation for each block. For block 1:

$$-c_p \cdot m_1 \cdot \frac{dT_1}{dt} = h_1 \cdot A_{surface} \cdot (T_1 - T_\infty) + \frac{A_{contact}}{R''_{Total}} \cdot (T_1 - T_2) \tag{2.2.5}$$

for block 2:

$$-c_p \cdot m_2 \cdot \frac{dT_2}{dt} = h_2 \cdot A_{surface} \cdot (T_2 - T_\infty) + \frac{A_{contact}}{R''_{Total}} \cdot (T_2 - T_1) \tag{2.2.6}$$

The initial conditions for the differential equations were the initial temperatures of the blocks:

$$T(o) = T_{initial} \tag{2.2.7}$$

The solution is similar to the one given by Kreith and Bohn (1997). The above first order differential equations can be combined into a single second order differential equation. Then from the initial block temperatures, the temperature time response can be predicted. The derivation of the solution follows.

Equations 2.1.5 and 2.1.6 can be rewritten, using the D operator to represent the derivative:

$$(D + \frac{A_{contact}}{R``_{Total} \cdot c_p \cdot m_1} + \frac{h_1 \cdot A_{surface}}{c_p \cdot m_1}) \cdot T_1 = (\frac{A_{contact}}{R``_{Total} \cdot c_p \cdot m_1}) \cdot T_2 + (\frac{h_1 \cdot A_{surface}}{c_p \cdot m_1}) \cdot T_\infty \tag{2.2.8}$$

$$(D + \frac{A_{contact}}{R``_{Total} \cdot c_p \cdot m_2} + \frac{h_2 \cdot A_{surface}}{c_p \cdot m_2}) \cdot T_2 = (\frac{A_{contact}}{R``_{Total} \cdot c_p \cdot m_2}) \cdot T_1 + (\frac{h_2 \cdot A_{surface}}{c_p \cdot m_2}) \cdot T_\infty \tag{2.2.9}$$

The equations can be simplified by defining:

$$K_1 = \frac{A_{contact}}{R``_{Total} \cdot c_p \cdot m_1} \ , \ K_{12} = \frac{h_1 \cdot A_{surface}}{c_p \cdot m_1} \tag{2.2.10}$$

$$K_2 = \frac{A_{contact}}{R``_{Total} \cdot c_p \cdot m_2}, \ K_{22} = \frac{h_2 \cdot A_{surface}}{c_p \cdot m_2} \tag{2.2.11}$$

Solving eq. 2.1.5 for T_2 and eq. 2.1.4 for T_1:

$$T_2 = \frac{K_2 \cdot T_1 + K_{22} \cdot T_\infty}{(D + K_2 + K_{22})} \tag{2.2.12}$$

$$T_1 = \frac{K_1 \cdot T_2 + K_{12} \cdot T_\infty}{(D + K_1 + K_{12})} \tag{2.2.13}$$

Equations 2.1.4 and 2.1.5 can then be written solely in terms of the temperature of that block only and the ambient temperature parameter by substituting equations 2.1.12 into 2.1.8 and 2.1.13 into 2.1.9:

$$(D + K_1 + K_{12}) \cdot T_1 = K_1 \cdot \frac{K_2 \cdot T_1 + K_{22} \cdot T_\infty}{(D + K_2 + K_{22})} + K_{12} \cdot T_\infty \tag{2.2.14}$$

$$(D + K_2 + K_{22}) \cdot T_2 = K_2 \cdot \frac{K_1 \cdot T_2 + K_{12} \cdot T_\infty}{(D + K_1 + K_{12})} + K_{22} \cdot T_\infty \tag{2.2.15}$$

Equation 2.1.10 and 2.1.11 can be written in non-operator notation as:

$$a_1 \frac{d^2 T_1}{dt^2} + b_1 \frac{dT_1}{dt} + c_1 T_1 = d_1 \cdot T_\infty \tag{2.2.16}$$

$$a_2 \frac{d^2 T_2}{dt^2} + b_2 \frac{dT_2}{dt} + c_2 T_2 = d_2 \cdot T_\infty \qquad (2.2.17)$$

Where:

$$a_1 = 1; \qquad b_1 = K_2 + K_{12} + K_{22} + K_1; \qquad (2.2.18)$$

$$c_1 = K_1 \cdot K_{22} + K_{12} \cdot (K_2 + K_{22}); \qquad d_1 = K_1 \cdot K_{22} + K_{12} \cdot (K_2 + K_{22})$$

As the systems are thermally equivalent, it is apparent that the parametric expressions for the differential equations (2.1.16) and (2.1.17) are equal so that:

$$a_1 = a_2; \qquad b_1 = b_2; \qquad c_1 = c_2; \qquad d_1 = d_2 \qquad (2.2.19)$$

The value of the constants *a, b, c* and *d* for the two blocks would vary, as the masses, surface areas and loss coefficients could vary, but the parametric expressions would not. In the experiments, identical blocks were used, and the numerical value of the constants were equal.

The system of two first order differential equations has been converted into one second order differential equation. The conversion of both block equations has been shown, but only one conversion would be needed to solve for the temperature of both blocks as a

function of time. Once one block temperature was determined, the other could be found from substitution into eq. 2.2.14 or 2.2.15.

As the differential equation for each block is non-homogenous and second order, it requires both a general and a particular solution. The use of subscripts denoting each block has been dropped, as the derivation is the same for each block. The homogenous solution to 2.1.12 and 2.1.13 is:

$$T_h = C_1 e^{m_1 * t} + C_2 e^{m_2 * t} \tag{2.2.20}$$

m_1 and m_2 are the roots of the characteristic equation for each block. Assuming real, unequal roots:

$$m_1 = \frac{-b + \sqrt{b^2 - 4 \cdot a \cdot c}}{2 \cdot a} \tag{2.2.21}$$

$$m_2 = \frac{-b - \sqrt{b^2 - 4 \cdot a \cdot c}}{2 \cdot a} \tag{2.2.22}$$

The particular solution for the differential equation is:

$$T_p = C_3 \tag{2.2.23}$$

The complete solution is:

$$T = C_1 e^{m_1 * t} + C_2 e^{m_2 * t} + C_3 \tag{2.2.24}$$

The initial temperature of each block is established from measurement, and the first derivative is defined from equations 2.2.5 and 2.2.6. The initial conditions are:

$$T_i = T_o \qquad \text{at } t = 0 \tag{2.2.25}$$

$$\frac{dT_i}{dt} = \frac{-1}{m * cp}(h_i \cdot A_{surface} \cdot (T_i - T_\infty) + \frac{A_{contact}}{R''_{Total}} \cdot (T_i - T_j)) \qquad \text{at } t = 0 \tag{2.2.26}$$

C_1, C_2 and C_3 are found from:

$$T_o = C_1 + C_2 + T_\infty \tag{2.2.27}$$

$$\frac{-1}{m * cp}(h_1 \cdot A_{surface} \cdot (T_i - T_\infty) + \frac{A_{contact}}{R''_{Total}} \cdot (T_i - T_j)) = C_1 \cdot m_1 + C_2 \cdot m_2 \tag{2.2.28}$$

where T_i and T_j are the initial block temperatures.

Equations 2.1.23 and 2.1.24 are two independent equations with two unknowns, which can be simultaneously solved for both C_1 and C_2. Once the constants are known, eq 2.1.20 can be used to predict the temperature time response of the two blocks.

2.3 Experimental Equipment

The important independent parameters of the experiment are the thermal conductivity of the interface plastic, the surface roughness, flatness and mass of the blocks in contact, the interface pressure, and the loss characteristics of the insulating material.

Aluminum blocks were chosen, due to their ready availability as well as ability to be accurately machined. In addition the high thermal conductivity of aluminum (170 W/m-K) reduced the temperature gradients within each block. The blocks were machined to a surface roughness of 2.5 x 10^{-7} m Ra, close to the surface finish found on production Thermalon®(1-5 x 10^{-7} m). A representative surface scan of one of the blocks is shown below.

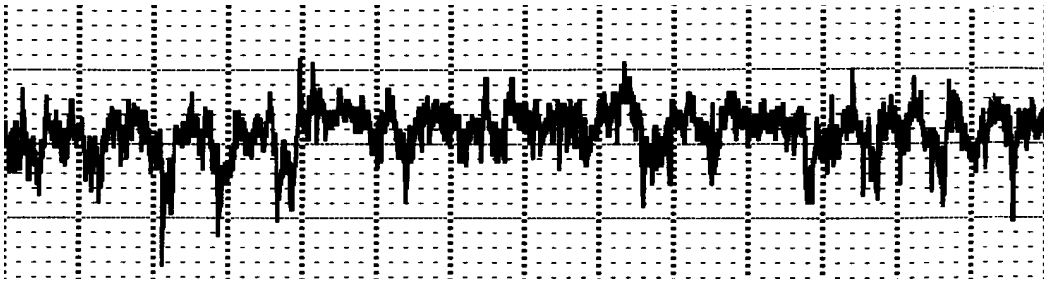

Figure 2.3.1: Representative Block Surface Profiles.

On the vertical axis, each of the four major vertical divisions is $1x10^{-6}$ m, or $3.93x10^{-5}$ in. On the horizontal axis each major division is $1x10^{-5}$ m. The average roughness for the surfaces is 0.20 μm.

Expanded polystyrene solid cell insulation, having a thermal conductivity approximately equal to 0.029 W/m-K was used to make the insulation enclosing the blocks and the plastic. The insulation was split into three pieces to totally enclose the block system, as shown in figure 2.3.2 below.

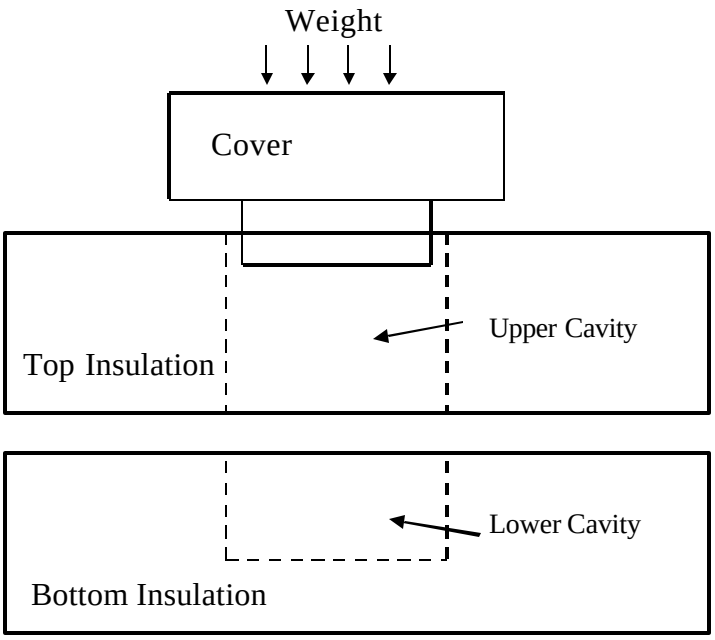

Figure 2.3.2: Block Insulation System.

An Omega Dyna-Res Data Acquisition System was used in this study to record the temperature measurements. It has 16 channels and 16 bit resolution on the analog inputs. Quick Log PC, also by Omega, was used as the data logging and control software. A lab 486

computer running Windows 95 was the host computer. Type ‘T’ thermocouples were used, with an accuracy of 0.7 °C relative to ambient. The hot block and cold block thermocouples track together to a maximum error of 0.3 °C over the range of the test conditions. The tracking error determined the error in the measurements as the change in energy of the blocks was needed, and systematic errors in the measurements, due to the cold junction compensation for example, were cancelled out in the data reduction techniques.

Type T thermocouples were embedded in the blocks along the centerline at half the height of each block. Silicone sealant insured good thermal connection between the thermocouple and the block. Additional thermocouples were inserted in the insulation to determine the heat loss through the insulation through the environment. The signal conditioning board of the data acquisition system provided noise filtering and cold junction compensation for the thermocouples.

At the start of each experiment the cold block, which was approximately at room temperature, was placed inside the lower cavity of the bottom insulation. The plastic sample used to evaluate the contact resistance was cut into a circle to the same diameter of the aluminum blocks (7.62 cm). It was then placed on top of the polished surface of the cold block. The hot block was then heated with a propane torch to a temperature below the softening point of the sample being tested. Typically this was 60-80 °K above ambient. The hot block was then placed on top of the sample with the polished surface of each block towards the sample.

As quickly as possible the top insulation was placed around the hot block. The upper cavity had been cut larger than the block diameter to allow the top insulation to completely surround the hot block. The top cover was placed on top of the hot block. The cover was cut so that it entirely rested on the top block and had a small clearance to the sides of the top insulation. The additional weight needed to produce the required interface pressure between the two blocks was then placed on top of the cover. The entire system could be assembled in approximately 10 seconds after the top block had been placed on top of the cold block, minimizing the energy lost to the surroundings.

The energy lost through the insulation from both blocks varied from 3 to 20 % of the total energy transferred from the top block to the bottom block. The low energy losses were for the thin polypropylene sample where the hot and cold blocks equalized quickly. The higher losses occurred with the relatively thick embossed polyethylene where the high resistance between the blocks gave more time for them to leak heat to the ambient. In both cases this energy loss is accounted for by including the loss parameter in developing the differential equations. See section 2.1 for more information.

2.4 Data Reduction Technique

In order to determine the contact resistance, measured temperature – time response data is compared with the response predicted by the lumped thermal capacitance

approximation. The error between the measured block temperatures and the predicted temperatures was calculated at each time step. The total error for the run was then calculated as:

$$Error = \sum_{i=1}^{i=j} \sqrt{(T^{i}{}_{hp} - T^{i}{}_{hm})^2 + (T^{i}{}_{cp} - T^{i}{}_{cm})^2} \qquad (2.4.1)$$

Where h, c, p and m stand for hot, cold, predicted and measured respectively. *i* was the value at each time step, and *j* was the final time step. A least squares approach was used in order to minimize the sum of the absolute value of the error at each time step.

An optimization program written in EES (Klein and Alvarado 1998) was used to solve for the values of the parameters that yielded the 'best fit' of the analytical solution to the measured temperatures for each run. The error between the analytical solution and the measured values was minimized by varying the contact resistance, the initial temperatures of the two blocks and the loss coefficient of the blocks.

The value of the error had no intrinsic meaning, and was only a qualitative measure of how well the analytical solution fit the measured data. Smaller errors were better, but were not related to the experimental error in the contact resistance value. One hundred sample points, usually spaced at 2 second intervals, were used in each optimization run. Two hundred seconds of data was sufficient to show the exponential effect of the transient response and the losses to the ambient sink. Figure 2.4.1 below shows the both measured and

predicted hot and cold block temperatures during a test. The difference between the measured and predicted temperatures was used to find and reduce the error.

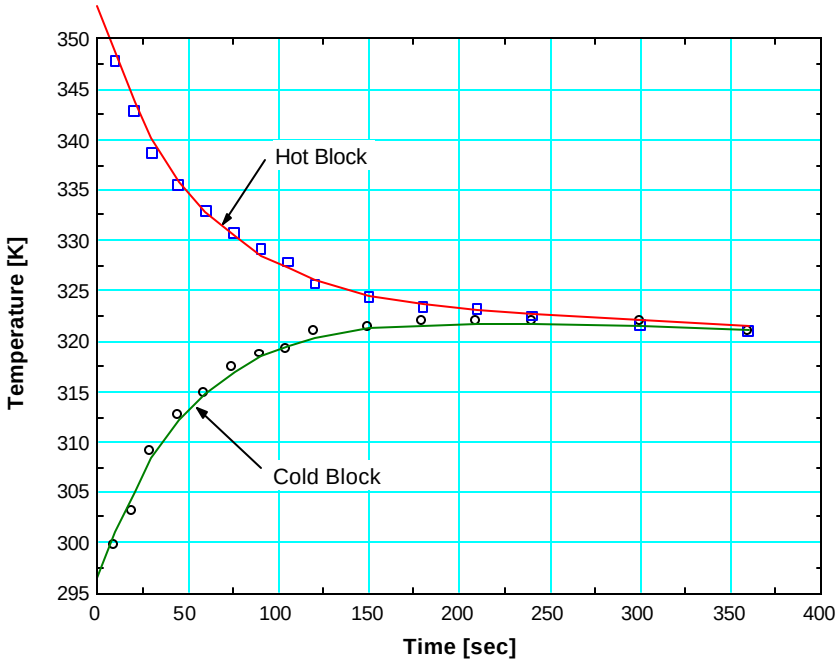

Figure 2.4.1: Predicted and Experimental Block Temperature Response.

Guess values and variable bounds were provided to the EES optimization routines. The guess values for temperature were taken from the measured temperature of the blocks, and the guess values for the loss coefficients and the contact resistance were extracted from the final results of the last run. The error for each run was quite sensitive to the varied parameters, and if the bounds of any parameters were unduly restricted a high error would result. A visual check of a plot of the best-predicted response and the actual measured temperature response of the two blocks was a good indicator of both whether the optimization had found the true minimum and how sensitive the reduction technique was to certain variables.

The figure 2.4.2 shows the effect on the predicted block temperature response of varying the contact resistance. For the ‘best fit’ case the temperature response follows the measured response very closely. With a contact resistance that is too low the blocks are predicted to come together too quickly. With a contact resistance that is too high, the blocks take too long to reach equilibrium.

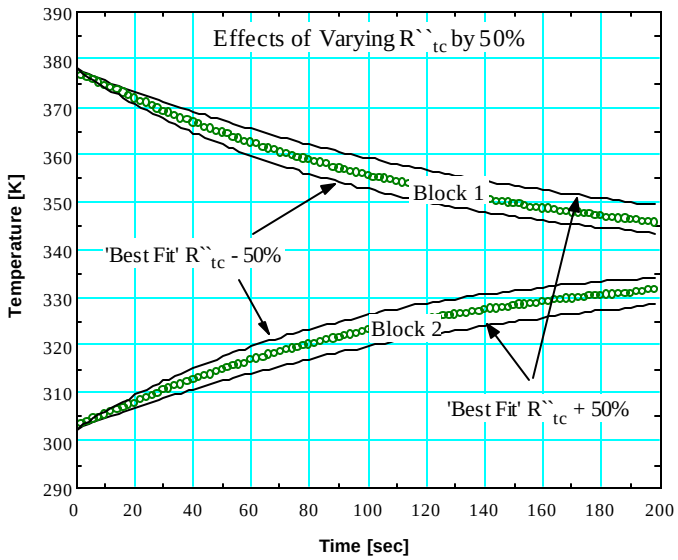

Figure 2.4.2: Predicted Block Temperature Response for Various Contact Resistances

Figure 2.4.2 is based on a 0.127 mm thick polyester run at an intermediate pressure (2-3 kpa). In the length of the test, 200 seconds, the blocks have come with in 15 °K of each other. For the same initial conditions and interface pressure, the blocks would have reached with in 5°K or 25°K of each other for the 0.0203 mm polypropylene and 0.0508 mm embossed polyethylene respectively.

The initial temperature proved to be a critical parameter in the optimization process. If the initial temperatures were assumed that were more than a degree or two off of the true optimum, bad fits could be created. In the plot below, this is clearly shown.

Underestimating the value of the initial temperature difference between the two blocks caused the optimization routine to overestimate the value of the contact resistance. This can be seen in the curves of the predicted responses in figure 2.4.3 where the predicted temperature response curves do not match the measured curves.

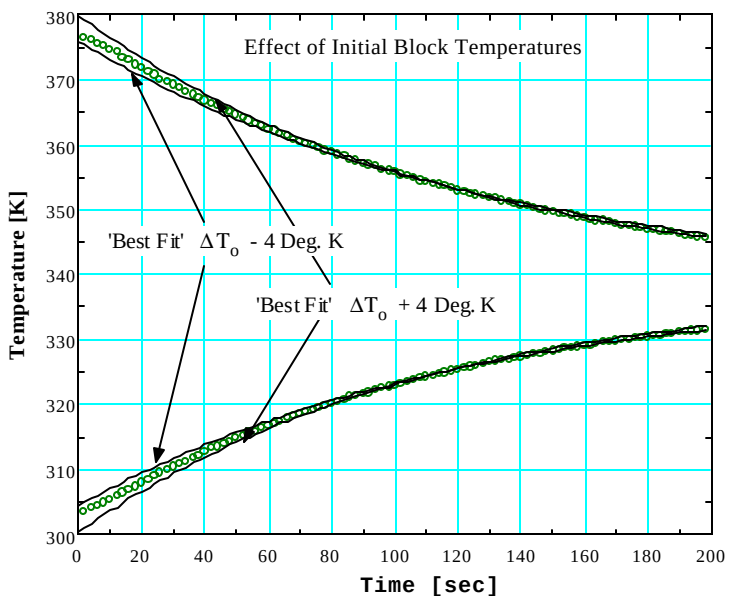

Figure 2.4.3: Effect of Initial Block Temperatures.

Due to the sensitivity of the best fit R_{tc} the initial temperatures of the block were varied by the optimization routine. Although the initial temperatures were measured with the data acquisition system, the actual temperature when the blocks were brought together and

the initial temperature used in the lumped capacitance response differential equation for the best fit could differ. Upon contact the blocks internal temperature profile takes time to establish. The temperature at the contacting surface of the bocks would be closer to each other than the temperature measured at the centerline of the blocks by a small amount. The lumped capacitance model by definition sees the blocks at a single temperature, so that temperature was treated as an unknown.

The actual loss parameter is measured by allowing both blocks to come to equilibrium and then recording the temperatures as the blocks cool to room temperature. Due to the difference in how the insulation was assembled around the blocks, each block had its own loss parameter. The loss parameter is assumed to be constant throughout each test.

2.5 Verification of Technique

Initial verification of the data reduction technique was accomplished by measuring the thermal conductivity of a known sample. Polystyrene in expanded bead form was used because it has a relatively low value of conductivity, and the thermal conductivity does not vary with temperature. Each side of the sample was coated with conductive grease, to reduce the contact resistance to essentially zero. The total resistance between the two blocks was measured and then the thermal conductivity of the polystyrene was deduced from the total resistance. The temperature response of the cold block for the first 400 seconds is shown in figure 2.5.1 below. The best-fit value of conductivity is 0.37 W/m-K in this test.

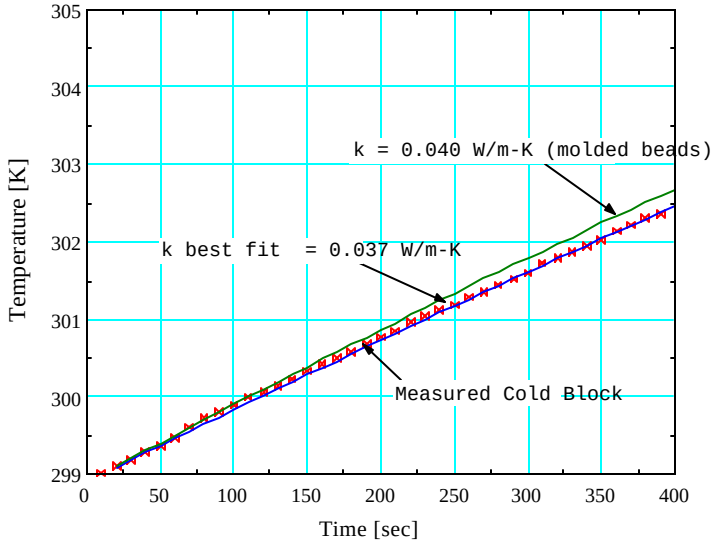

Figure 2.5.1: Polystyrene Conductivity Tests

The thermal conductivity of the polystyrene was measured repeatedly and found to vary 2.7 %. The thermal conductivity measured correlated to the accepted value given in Incropera and Dewitt (1996), to within 8%. There is however some variation in the published conductivity of polystyrene, with Osswald and Meneges (1996) giving a value 25% lower than the one given in Incropera and Dewitt.

Representative data was used to examine the effect of sampling periods on the determined contact resistance. Both the number of samples used in the data reduction and the initial time of the samples after the blocks were placed in contact were varied. Any systematic variation in the determined contact resistance would be due to an error in the data reduction method. Plots of the contact resistance determined are shown in figure 2.5.2 and

2.5.3 below. The time of reduction is shown on the x-axis, and the measured contact resistance is shown on the y-axis.

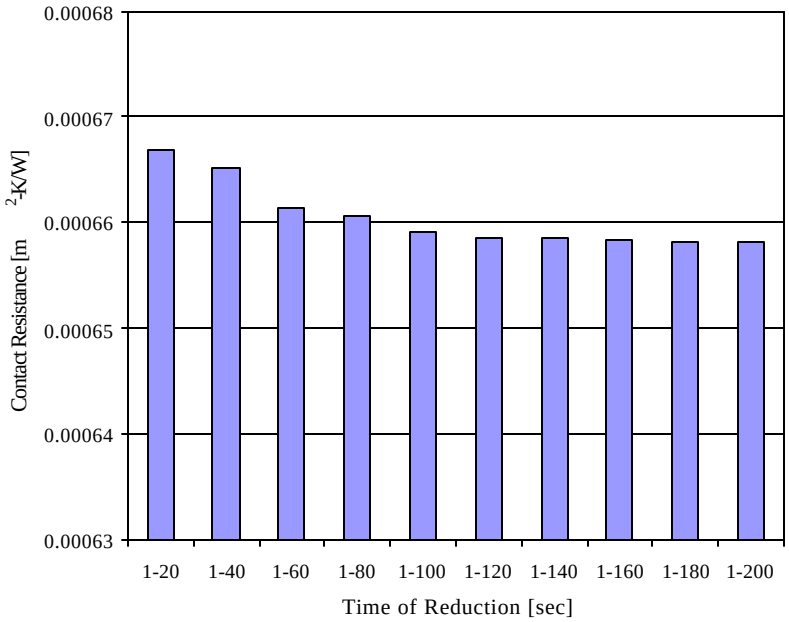

Figure 2.5.2: Determined Contact Resistance vs. Sample Time.

The resistance values are larger for small sample periods than they are for longer data runs, and reach an asymptote at approximately 100 seconds. This is due to the initial transient response of the conduction heat flows internal to each block. The heat flows internal to the block set up an internal temperature profile based on Fouriers' law of conduction. The time constant of the temperature profile development is much quicker than the time constant of the overall transient response of the hot and cold blocks together. All tests use at least 200 seconds of temperature data to ensure that the initial transients within each block are over. Additionally allowing the optimization routine to vary the initial temperatures reduces the effect of the initial transients.

If only twenty seconds worth of samples (10 actual samples) are used, but taken from different time periods in the measured response, there is a small variation in the measured contact resistance. The small variation is much less than the variation between tests for any of the samples and is probably due to thermocouple errors. Figure 2.5.3 shows the variation as a function of when the samples were taken in the test.

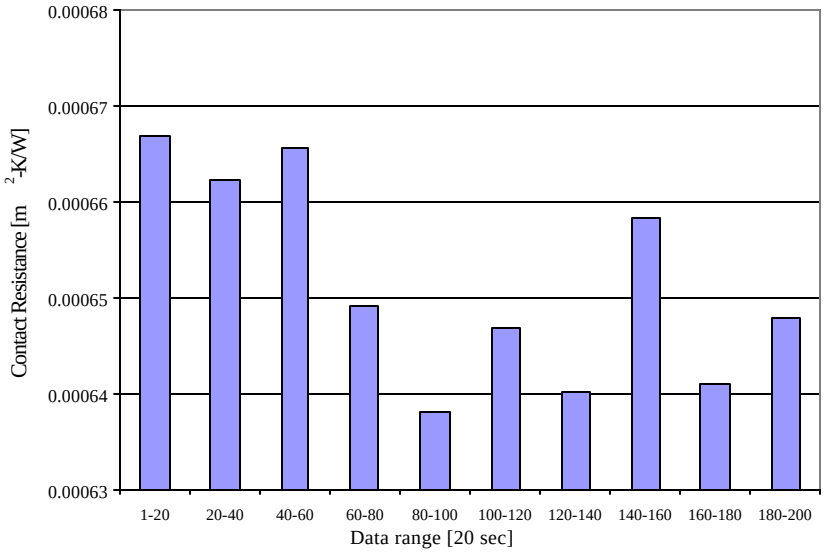

Figure 2.5.3: Determined Contact Resistance vs. Time after Initial Contact.

There is no pattern in the variation of the contact resistance based on the different sample times, and the standard deviation for the series is less than 2% of the measured contact resistance. For the data taken from the start of the test, the temperatures of the blocks would still be changing rapidly, after 100 seconds however the blocks temperature would be changing more slowly. The change in temperature at the start would be much greater than the

noise in the measurements, at the end of the measurement period the signal to noise ratio would be lower.

The Biot number parameter is critical to the assumption of thermally lumped mass. The Biot number is defined as the ratio of the resistance to conduction heat transfer through the solid to the resistance to heat transfer from the solid top the surroundings. At ratios less than 0.1, the solid can be thermally lumped. For the two blocks and the contact resistance, the Biot number was equal to:

$$Bi = \frac{R''_{internal}}{R''_{external}} = \frac{L_{block}}{2 \cdot k_{aluminium} \cdot R''_{total}} \tag{2.5.1}$$

Where L_{block} is the height of each block. For any run where the Biot number parameter was not less than 0.1, a lumped capacitance approach was not applicable. As the Biot number was based on the total resistance between the two blocks, the conduction resistance of the plastic sample was important in the Biot parameter. For some of the thin polypropylene samples the Biot numbers approached 0.1, and a different approach had to be found for the data reduction. The distributed capacitance technique is described in the next section.

2.6 Finite Difference Technique

A distributed capacitance technique was used to examine the limits of the lumped capacitance technique as well as the effect of the capacitance of the insulation on the

experiments. A two dimensional transient finite difference program was written to model the heat flows through the blocks, the plastic sample and the surrounding insulation. The distributed capacitance technique had some advantages over the lumped capacitance technique. It accounted for the internal temperature profile within the blocks, accommodated the difference in temperature between the thermocouple insertion point and the surface temperature of the blocks, and allowed insulation to be modeled as having a distributed thermal capacitance.

Analytical solutions like the lumped capacitance method are difficult to obtain when systems become more complex with non-ideal characteristics. Various numerical methods have been used to solve differential equations over irregular boundary conditions. For conduction heat transfer the finite difference is the most straightforward and easiest to apply. With the finite difference method, the domain under consideration is divided into discrete volumes, with each volume having a singular temperature representing the average temperature of the whole volume. The solution to the difference equation is found at those discrete points, and the system of equations describing all of the nodes in the domain is solved simultaneously.

The differential equation of interest is Fourier's law of heat conduction, usually written as:

$$q``_x = -k_x \frac{\partial T}{\partial x} \tag{2.6.1}$$

Using the definition of the derivative and discretizing the numerical derivative is:

$$q``_x = -k_x * \left(\frac{T_{x+\frac{\Delta x}{2}} - T_{x+\frac{\Delta x}{2}}}{\Delta x}\right) \qquad (2.6.2)$$

The temperature gradient is based on temperatures found at the nodal points used in the domain mesh. The transient energy balance for each node is written using the first law of thermodynamics, as was done with the lumped capacitance technique, see equation 2.1.2. The finite difference form of the conduction heat flows including storage is shown below:

$$m * cp * \frac{dT}{dt} = \frac{a_x * k_x}{\Delta x} * (T_{x+\Delta x} + T_{x-\Delta x} - 2 * T_x) + \frac{a_y * k_y}{\Delta y} * (T_{y+\Delta y} + T_{y-\Delta y} - 2 * T_y) \qquad (2.6.3)$$

Equation 2.6.13 has been discretized in space but not time. The first order differential equation can then be integrated with any applicable technique. See Anderson (1995).

2.7 Model Grid and Resistance Network

A model of the blocks, the plastic and the insulation was used in the formation of the finite difference code. The blocks and plastic were linked by an axial coordinate system running vertically through the test apparatus. The blocks were modeled with 5 nodes each and three nodes in the plastic sample. The blocks were thermally linked with the insulation by assuming each vertical section of block was at a constant temperature and conducted heat

outward radially. The insulation surrounding the blocks was modeled using a radial coordinate system, with three nodes in an outward direction. The insulation was divided up into vertical slabs of the same thickness as the block slabs, and the conduction resistance between the inner nodes in the insulation and the block nodes was equal to the conduction resistance in the insulation and the blocks. Figure 2.7.1 below shows a schematic of the thermal resistance network modeled in the distributed capacitance analysis.

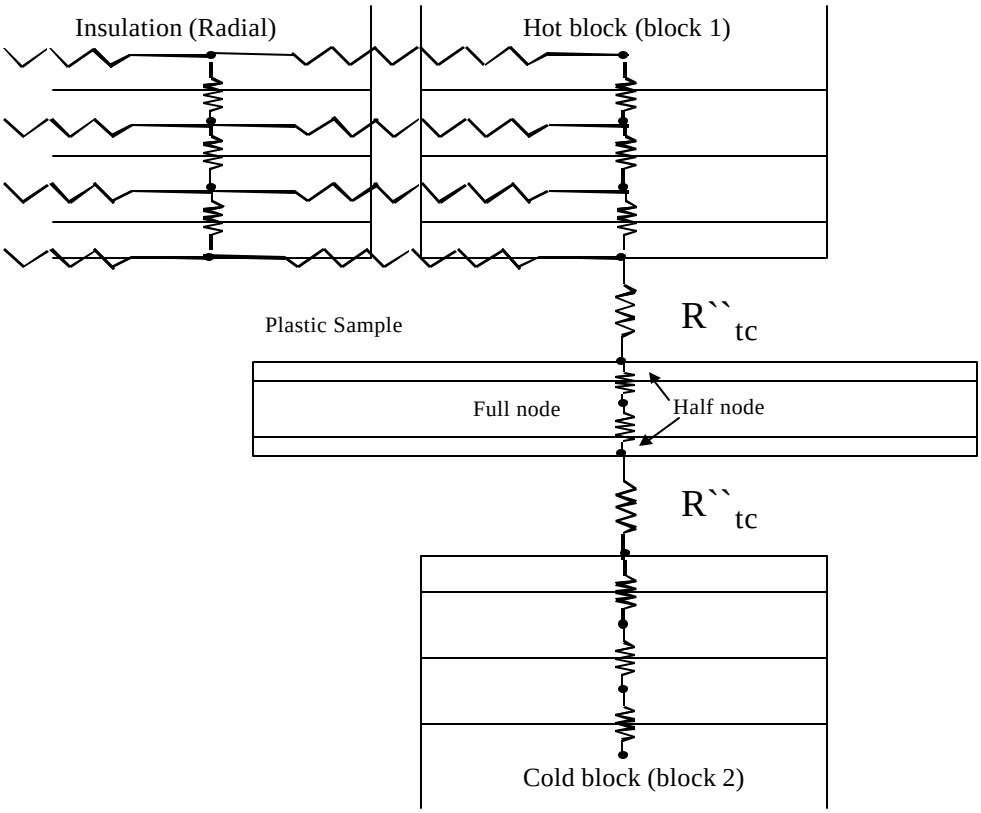

Figure 2.7.1: Distributed Capacitance Model Schematic.

Although not shown in figure 2.7.1, there were also radial insulation nodes wrapped around the bottom block. The aluminum blocks were divided into ‘slices’ with each slice being represented by a single temperature at the nodal point. The actual resistance between the nodes of the blocks and the insulation was set to the total of the conduction resistance of the aluminum slice and the conduction resistance of the insulation. As the expended bead polystyrene insulation had approximately the same thermal conductivity as air (0.032 W/m-K for polystyrene and 0.029 W/m-K for air), the contact resistance between the insulation and the aluminum block was negligible.

The integration scheme must be used to model the energy inflows and outflows over time. The program was written using EES, and the INTEGRATE function was used to predict the changes with time. EES uses a second-order predictor-corrector algorithm for evaluating the integral, and the automatic step size function was used. The temperature of any given aluminum node i , in the block was given as;

$$T^{i}(t) = T_{o}^{i} + \frac{1}{m_{node} * cp_{al}} * \int_{t=0}^{t} \left(\frac{a_{y} * k_{al}}{\Delta y} * (T^{i+1}(t) + T^{i-1}(t) - 2 * T^{i}(t)) + q_{insulation}\right) \partial t \quad (2.7.1)$$

Figure 2.7.2 below shows the top and bottom node temperatures predicted by the finite difference model. A reference case of an average contact resistance and a polyester sample are shown. The top and bottom node of the hot and cold blocks, as well as the top and bottom node of the plastic sample is also shown.

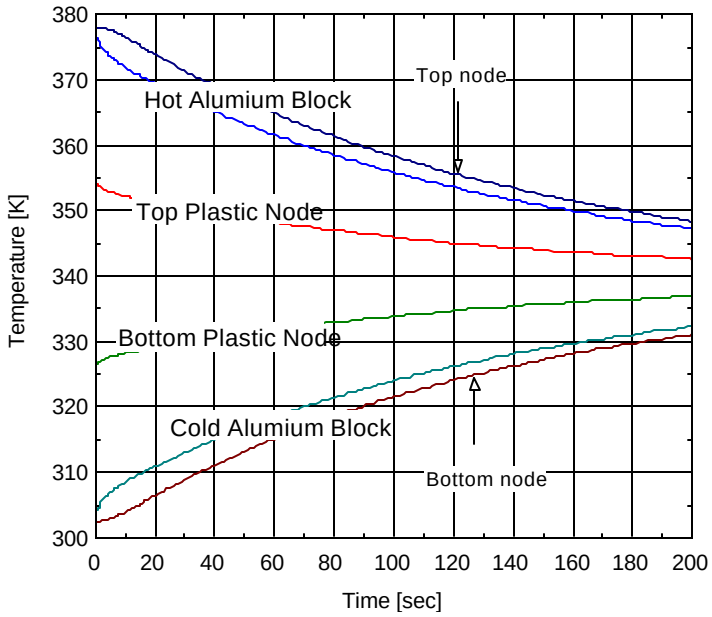

Figure 2.7.2: Predicted Temperature Contours for Polyester Sample, $R_{tc} = 0.0007\ m^2\text{-}K/W$

The temperature distribution through the blocks and the plastic can be clearly seen. The cold block is absorbing energy from the hot block and heating up. The plastic temperature is at the average of the inside surface temperatures of the two blocks, and stays relatively constant throughout the tests. The temperature drop across the block and the plastic, which is due to the contact resistance, can also be seen. The thermocouple insertion points used in the actual experiments were half way up the blocks and would be between the top and bottom node temperature extremes shown for each block. The cooling due to the heat loss through the insulation is hard to discern on the plot, and has little effect on the measurements.

The relative temperature drops from surface to surface determine the resistances in the system. The three temperature drops from the aluminum surface to the top plastic surface, through the plastic from the bottom plastic to the top aluminum surfaces are roughly equal. The equal temperature drops mean that the plastic properties must be well known to achieve an accurate measurement.

The temperature profiles within the blocks can best be seen by plotting the nodal temperatures for each block. As the blocks are put together they quickly assume an internal temperature profile. The sharpest gradients at the start of the test and the smallest gradients as the blocks approach each other in temperature. Figure 2.7.3 below shows the predicted temperature gradients in the cold block during a typical run.

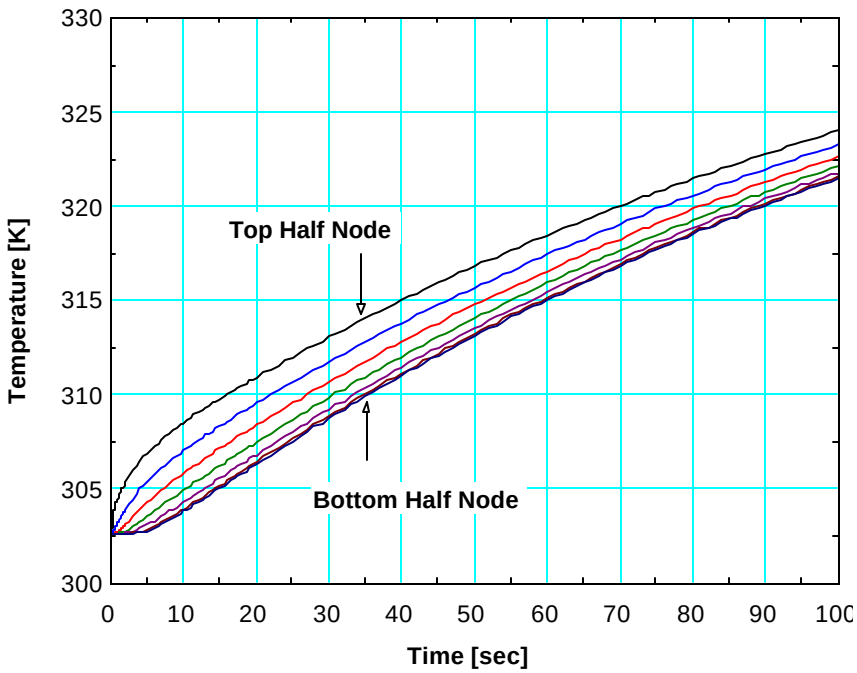

Figure 2.7.3: Predicted Temperature Differences at Nodal Locations Through Cold Block

The cold block starts out isothermal at the start of each test. After about 10 seconds however, the block assumes a temperature difference of about 7 degrees K from top to bottom. This temperature difference within each block decreases throughout the test as the temperature difference between the hot and the cold blocks decreases.

2.8 Biot Limit Effects

Using contact resistances found at the extremes of the study, the predicted temperature responses of the blocks were compared with the lumped and distributed capacitance systems. When the distributed capacitance method was compared with the lumped capacitance technique, the results were close, with a small error at a low contact resistance. Figure 2.8.1 shows the ratio of the temperature difference of the blocks divided by the initial temperature difference for both the lumped and the distributed capacitance technique. Two different contact resistances are used to illustrate Biot number effects.

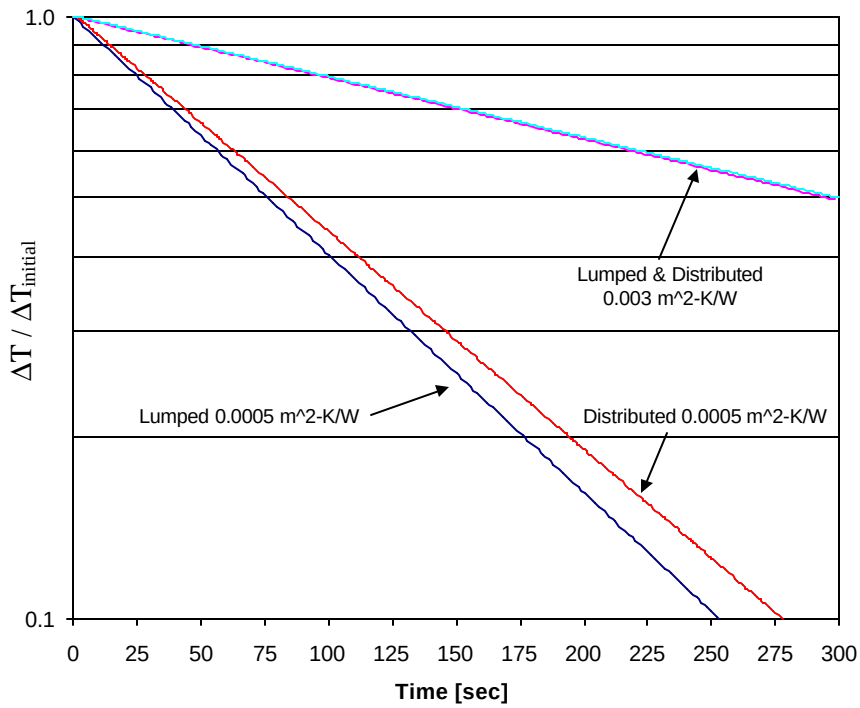

Figure 2.8.1: Comparison of Predicted System Response for Lumped and Distributed Systems.

Both methods are used to interpret measured block response data, but they interpret the data in different ways. Looking at how they predict the block response given a contact resistance value shows how well they will interpret block response data. In figure 2.8.1, the predicted response for two contact resistances at the extremes of the study are shown. For the contact resistance measured with the embossed polyethylene, 0.003 m^2-K/W, the two methods predict the same temperature response. At 0.0005 m^2-K/W, the predicted responses differ substantially. The lumped capacitance method predicts a quicker response (more negative response slope) by the two blocks. This is due to the driving potential defined by the contact resistance.

The contact resistance is defined as:

$$R''_{tc} = \frac{T_{hot} - T_{cold}}{q''} \tag{2.8.1}$$

The joint temperatures used by the lumped and distributed capacity technique differ slightly, affecting the measurements. The lumped capacitance technique defines the driving potential across the average temperature of the two blocks, whereas the distributed capacitance defines it across the slice of block in contact with the plastic. As the average temperature difference is greater than the temperature difference across the contact surfaces, for the same contact resistances there will be higher heat flow for the distributed case and the blocks will equilibrate faster.

When the contact resistance is being measured based on recorded temperature data, the lumped capacitance technique will predict a higher contact resistance than the distributed capacitance method. The same heat flow between the blocks is seen, and the distributed capacitance method will see a lower driving temperature potential across the interface and will then find a smaller contact resistance.

For an actual joint contact resistance of 0.0005 m^2-K/W, the difference between what was measured by the lumped capacitance technique and the distributed capacitance technique

would be 20%. The distributed capacitance technique would still over predict the contact resistance, but by a much smaller amount. For this reason, the contact resistance of the relatively thin polyester and polypropylene plastics was calculated using the distributed capacitance analysis.

The above error analysis would not have been possible without the distributed capacitance model. The plane wall corrections available in the literature Heisler (1947) are not strictly applicable given the transient nature of the sink temperature for each block, i.e. the other block.

There was also the Biot parameter for the ratio of the resistance inside each block to the resistance to the surroundings. The Biot parameter for convection proved much smaller than the Biot parameter for the total resistance and was on the order of 2×10^{-5}.

2.9 Heat Flows In Insulation

For the lumped capacitance model of the static block test equipment, the losses to the surrounding insulation were modeled with a constant loss coefficient. A constant loss coefficient was an idealization as the insulation has a distributed thermal capacitance of its own, and its low conductivity may give rise to transient temperature effects in the insulation. In the formulation of the finite difference model of the blocks, plastic and insulation, the

temperature distribution in the insulation was explicitly determined. The temperatures were modeled in each of the concentric insulation rings around the aluminum slices.

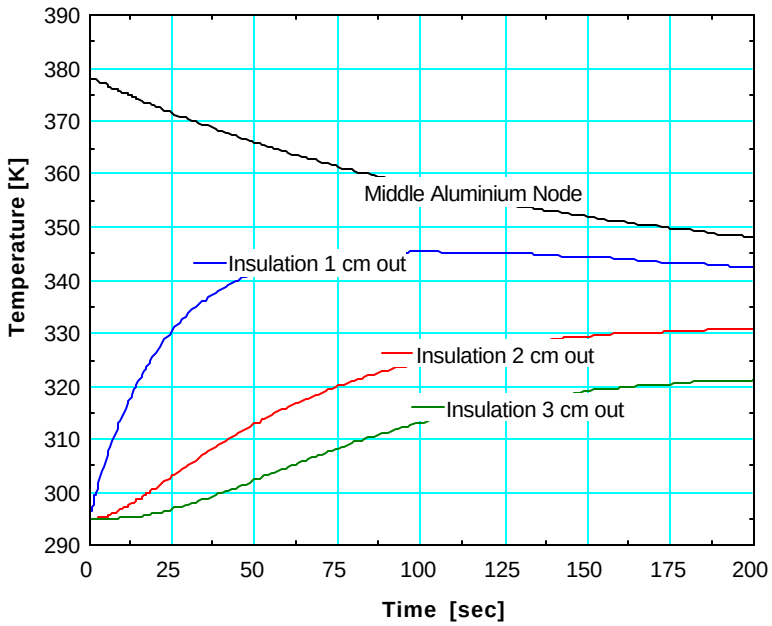

Figure 2.9.1: Predicted Insulation Temperature Response for Test Case.

Figure 2.9.1 shows the temperatures in the concentric insulation around the middle aluminum node in the hot bock. Each full slice in the aluminum block has a corresponding insulation layer. The middle aluminum node temperature is also shown for reference. As expected, the insulation ring closest to the aluminum node heats up the fastest. As the aluminum node is cooling due to the heat loss to the cold block, its temperature is decreasing as well. After 180 seconds, the aluminum block has cooled to close to the insulation temperature. If it went below the insulation temperature, energy would then flow from the insulation back to the block.

A comparison of the predicted and actual energy losses in the test apparatus was performed. The actual energy loss to the ambient per time step was measured by finding the change in the average temperature of the blocks from one time step to the next. Ideally all energy should be transferred between the blocks, and none lost to the environment. The lumped capacitance technique considered each block to have a constant loss coefficient, and the distributed considered each block slice to be conducting out to its surrounding insulation.

Figure 2.9.2 below shows the measured heat losses during a block test with a 0.127 mm polyester sample. In addition the predicted losses from the lumped and distributed capacitance methods is also shown. The assumption of a constant heat loss parameter approximates the data better then the distributed capacitance method does. The better fit is partially due to allowing the loss coefficients to be 'best fit' to the data during reduction. The 'best fit' convection coefficients were determined to be 6.7 and 2.9 W/m^2-K, for the top and bottom block respectively. The difference is expected due to the way the insulation is placed together during an experiment. The cold block is enclosed in a single piece of tightly fitting insulation, and the hot block is more exposed during the test. For a schematic see figure 2.2.1. The conductivity of the insulation was 0.029 W/m-K, based on manufacturer specifications.

The ratio of energy lost to the environment to energy transferred to the cold block in this experiment was 9.8 %. The average heat loss ratio in the polypropylene runs was 1-3 % and for the embossed polyethylene it was approximately 15%. As the energy loss was

accounted for in either of the models used, it had little effect on the accuracy of the contact resistance measurements.

The predicted heat losses to the insulation were compared with the measured losses. The scatter in the measured loss data shown in figure 2.9.2 is due to the sampling error and noise in the thermocouple and data acquisition system.

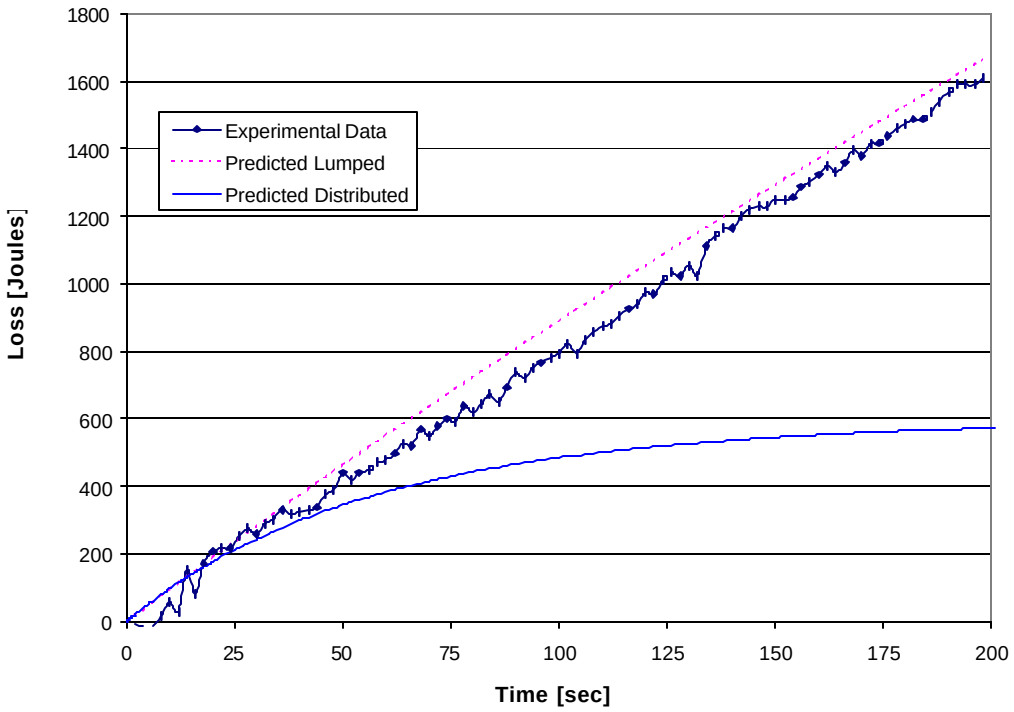

Figure 2.9.2: Predicted and Experimental Energy Losses.

The distributed capacitance technique does not do an adequate job of predicting the heat losses to the environment. It matches the measured losses until approximately 50 seconds into the tests, and then diverges. The distributed capacitance model shows a transient

effect to the heat loss that is not shown in the data. It is unexpected that the rate of the losses (Watts) from the blocks was almost constant. Although the average temperature and internal energy of the two blocks are almost constant throughout the test, energy is begin transferred to the cold block, which has a much lower convection coefficient. The average measured heat losses at the start and end of the polyester tests were 9.7W and 7.4W respectively.

2.10 Combination of Models

The final result of the model comparison was that the distributed capacitance method was the most accurate model of the block-plastic system, except for the energy losses. However it was relatively easy to change the distributed capacity insulation from the model and use a constant heat loss mechanism equation with the distributed capacitance model. The aluminum conduction to the insulation was changed to a convective loss to the ambient temperature. The heat loss coefficients could then be ‘best fit’ to the data for each run as they had been in the lumped capacitance system. The loss coefficients for each run were best fit using a least squares approach as done with the lumped capacitance approach.

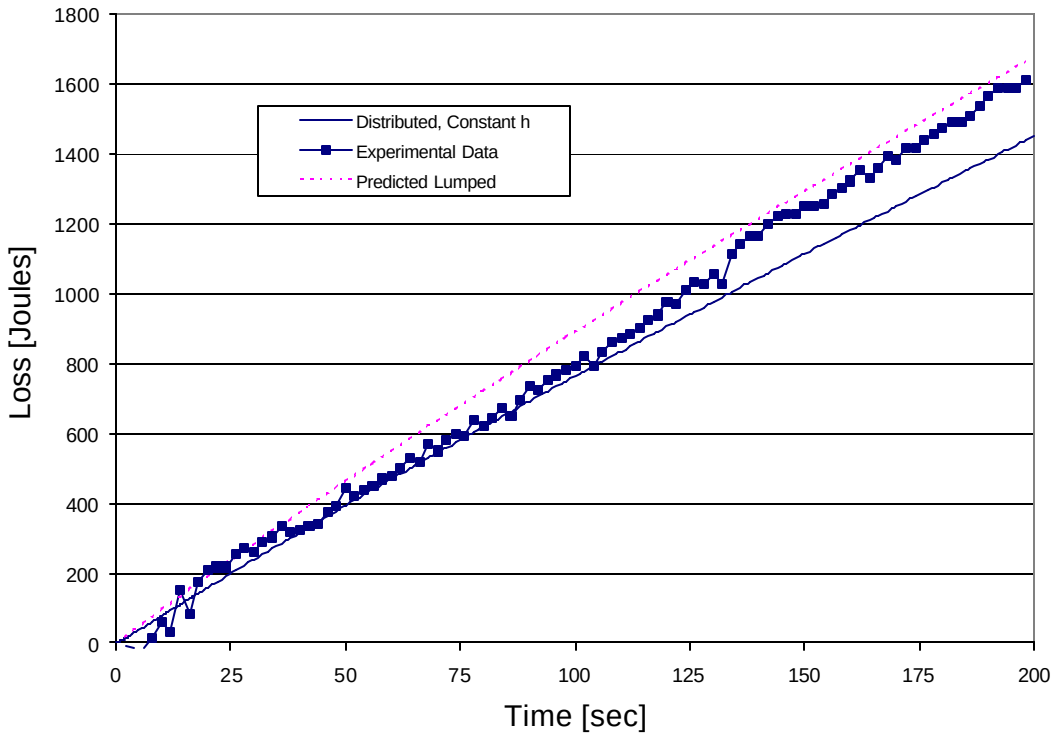

Figure 2.10.1: Predicted and Experimental Energy Losses.

As seen in figure 2.10.1, the predicted losses could be adjusted with the convection coefficients to accurately match the losses shown in the data. A comparison of figure 2.9.2 and 2.10.1 shows how much closer the constant loss model was. The 'best fit' convection coefficients were similar to ones measured in the lumped capacitance case, between 6-8 and 2-4 W/m^2-k for the top and bottom block respectively.

Once the analysis techniques were perfected for the range of data recorded, the time-temperature data could be reduced for each experimental run. Those results are shown in the next chapter.